

Self-assembly of core-corona particles confined in a circular box

Erik R. Fonseca and Carlos I. Mendoza*

November 6, 2021

Instituto de Investigaciones en Materiales, Universidad Nacional Autónoma de México, Apdo. Postal 70-360, 04510 CdMx, Mexico

Abstract

Using Monte Carlo simulations, we study the assembly of colloidal particles interacting via isotropic core-corona potentials in two dimensions and confined in a circular box. We explore the structural variety at low temperatures as function of the number of particles (N) and the size of the confining box and find a rich variety of patterns that are not observed in unconfined flat space. For a small number of particles ($N \leq 6$), we identify the zero-temperature minimal energy configurations at a given box size and we construct the phase diagram as function of temperature and box radius for the specific case of $N = 4$. When the number of particles is large ($N \geq 100$), we distinguish different regimes that appear in route towards close packing configurations as the box size decreases. These regimes are characterized by the increase in the number of branching points and their coordination number. In contrast to the case of confined hard disks, we obtain open structures with unexpected highly anisotropic character in spite of the isotropy of the interactions and of the confinement. Our findings show that confined core-corona particles can be a suitable system to engineer particles with highly complex internal structure that may serve as building blocks in hierarchical assembly.

1 Introduction

The search of particles on the mesoscopic scales that self-organize into potentially useful structures by virtue of their mutual interactions is extremely important since they can be used as building blocks for bottom-up nanofabrication processes [1, 2]. This is a large and rapidly growing field of tremendous technological potential and fundamental interest that has been fed by the continuing progress in the manipulation of the interaction potentials between nanoparticles [3]-[5].

*E-mail: cmendoza@materiales.unam.mx

Successful self-assembly of a structure depends not only on the interactions between the components as other factors intervene, for example reversibility, to allow the components to adjust their position within a structure, the thermal motion usually required to provide movement to the components and the environment where the components move.

In past decades, it has been recognized that one important factor affecting the assembly of particles is confinement. A significant amount of scientific attention has been devoted into the self-assembly of colloidal systems in different types of confinement. This interest is partly due to important problems in biosciences that involve objects confined inside a cavity [6]. To mention just a few, DNA packaging in viral capsids [7], macromolecular crowding in the cell [8], blood clotting [9] and pattern formation in biological structures [10]. Additionally, systems of physical relevance like the growth of colloidal crystals under confinement [11]-[14], the transport of particles in channels [15, 16] and others have contributed to the interest in studying the arrangement of particles under these conditions. As a result, the study of confinement has been used not only as a way to understand the behavior of the confined objects but as a general way of tuning colloidal self-assembly [17]-[22].

Most monodisperse colloidal particles are spheres. Thus, one problem in building new mesoscale ordered materials is controlling how spheres pack. Confinement of particles within containers such as micro-patterned holes or spherical droplets produce unexpected polyhedra that may become building blocks for more complex materials [23, 24].

In most cases, colloidal crystals found in confinement are close-packed. This can be a desired characteristic in problems related to efficient manufacturing, packaging, and transport [12]. However, one of the major goals in colloidal self-assembly is to devise new colloidal systems to self-assemble into low-density open crystalline structures [25, 26] which are partially due to their promising applications in photonics [27], catalysis [28], porous media [29] and the special response to mechanical stress [30]-[32]. Assemblies in the form of two-dimensional open networks are also of particular interest for possible applications because well-defined pores can be used for the precise localization and confinement of guest entities such as molecules or clusters, which can add functionality to the supramolecular network [33]. Two-dimensional packings of hard spheres under circular confinement results in optimal circle packings forming doublets, triangles, squares, pentagons, and hexagons [34]. It has been recently demonstrated by numerical simulations that soft particles described by the Daoud-Cotton model for star polymers assemble open structures in two dimensions [25]. Here we use computer simulations to investigate the self-assembly in two dimensions of particles consisting of a hard core surrounded by a soft corona that are confined in a circular box and the possibility to use confinement as a tool to control the final self-assembled structure, in particular, to obtain open arrangements and to engineer composite particles with non-trivial internal structure. Such non close packed supra-particles could be used as a mask for patterning or directly as a functional component for nanoscale applications. Although we consider only two-dimensional systems, similar behavior is expected in a three-

dimensional system of core-corona particles confined in a spherical box.

Particles interacting through core-corona potentials represent not only a simple model system to study numerically, such simple pair potentials are often used to describe effective interactions among substances with supramolecular architecture [35, 36]. For example, the case of diblock copolymers, dendritic polymers, hyper-branched star polymers, colloidal particles with block-copolymers grafted to their surface where self-consistent field calculations lead to effective interactions that can be modeled by a square-shoulder potential [37]. Such interactions can be controlled by adjusting the length, the grafting density of the grafted polymers, the quality of the solvent, etc. Also, isotropic core-softened potentials have been used to qualitatively describe the anomalous behavior of water and some other liquids and the effects that confinement have on the phase diagram [38].

Numerical simulations in flat space have shown that single component softened-core repulsive potentials may give rise to strip phases [39]-[43] and periodic structures that are explained in terms of the competing interactions between the hard core and the soft shoulder. Our aim is to study the influence that the size of a circular confining box has in the domain formation when the particles are restricted to move in the interior of the confining box.

The paper is organized as follows. Section 2 presents the model and the details for the Monte Carlo simulation. In Section 3 we show some of the complex structures obtained, a phase diagram for particular values of the parameters and the evolution of the assembled structures as confinement increases. Finally, in Section 4 we present our conclusions.

2 Methods

We employ a simple model system that treats the interactions between soft nanoparticles in an effective way via an infinite hard core encircled by a soft repulsive shoulder. Specifically, our system consists of particles interacting through an isotropic pair potential composed by an impenetrable core of diameter σ_0 with an adjacent square shoulder with range $\lambda\sigma_0$,

$$V(r) = \begin{cases} \infty & r \leq \sigma_0 \\ \epsilon & \sigma_0 < r \leq \lambda\sigma_0, \\ 0 & \lambda\sigma_0 < r \end{cases} \quad (1)$$

r being the pair distance (see Fig. 1a). At large distances, the particles do not overlap and the interaction vanishes. The repulsive shoulder may model the steric repulsion between nanoparticles due to the overlap of brush-like surrounding coronas. Finally, at small separations penetration of the compact cores is very unfavorable and gives rise to the hard-core repulsion. The simple functional form of the interaction potential not only captures the essential features of colloidal particles with core-corona architecture, it also offers many computational

advantages and allows to understand using simple geometrical considerations the system's self-assembly strategy [44, 45].

We consider that the nanoparticles are confined to move in a two-dimensional (2D) plane region limited by a circular disc of radius R as depicted in Fig. 1b. Standard Monte Carlo simulations based on the canonical ensemble (NVT simulations) in a circular box of radius R have been carried out using the Metropolis algorithm. We have used σ_0 and ϵ as length and energy units, respectively, set $\lambda = 2$, and studied the pattern formation dependence on $R^* \equiv R/\sigma_0$, reduced temperature $T^* \equiv k_B T/\epsilon$, where k_B is the Boltzmann's constant; and the number of particles N . The structural diversity and phase behavior is explored in detail for small number of particles $N \leq 6$ although runs with other values of N are considered, with the largest value $N = 400$ as an example of a large system. In all cases, the system is first disordered at high temperature and then brought from $T^* = 1$ to a final temperature $T^* = 0.01$ through an accurate annealing procedure with steps of 0.01 for a given value of the box radius R . The radius is progressively reduced in steps of $0.01\sigma_0$ from an initial large value, chosen such that the particles can be contained in the box without overlapping of their coronas, up to a final value such that no more contraction of the box is possible due to steric effects. An auxiliary interaction potential between the particles and the confining circle, of the form $V_{box}(r) = \epsilon/(R - \lambda\sigma_0/2 - r)^2 \Theta(0.02\sigma_0 + r - R + \lambda\sigma_0/2)$, with $\Theta(x)$ the Heaviside step function, is used to ensure that the particles remain inside the box each time its radius R is reduced. An equilibration cycle consisted, for each temperature, of at least 1×10^6 MC steps, each one representing one trial displacement of each particle, on average. At every simulation step a particle is picked at random and given a uniform random trial displacement within a radius of $0.5\sigma_0$. The temperature vs box size phase diagram is obtained during the annealing process as follows: for a given box size R , and temperature T , the average energy of the system is obtained. Then, from the average energy vs T plot, the critical temperature where the system changes from an isotropic random configuration to the self-assembled structure is obtained as the point where the curve reaches a final energy value that does not change anymore under further cooling. This is done for all R starting from the largest, where the particles do not overlap, to the more compact one.

3 Results

In unconfined space, core-corona particles make a plethora of mesophases. Thus, we expect to obtain a large variety of interesting structural features for this simple model at low temperatures as it is put in evidence in Fig. 2, where a few of them are exhibited for a confined system with a very small number of particles $N = 4$, corona to core ratio $\lambda = 2$ and for different sizes of the confining box, as indicated. Panel (a) shows the most compact representatives of every kind of arrangement obtained in this case. Each configuration is the result of the system minimizing its free energy and differs from the others by the number

of corona overlaps. For the larger box size shown, the four particles adopt a configuration determined by the particles just touching without overlapping their coronas, thus its free energy is $E = 0$. As the confining box decreases its size, the system can no longer avoid some overlapping and will adopt the configuration or configurations that minimize the number of corona overlaps. The second configuration corresponds to an arrangement in which there is only one corona overlap for which $E = \epsilon$. This configuration with only one overlap persists under progressive shrinking of the confining box up to a point in which this situation can no longer be maintained and a configuration with two overlaps appears as shown by the third case in panel (a). Further decrease of the box size will produce progressively, configurations with three, four, and six overlaps. The case with five overlaps is impossible due to geometrical constraints. Notice that all the most compact configurations shown are strictly rigid, except the case with $E = 4\epsilon$, which consists of two rigid dimers, each one consisting of a pair of particles located at opposite sides of the box, just touching their coronas. Each dimer can rotate independently of each other within the constrain imposed by the steric repulsion between the cores. This is indicated by a green line joining the particles forming one of the dimers and the arrows indicate its relative movement with respect to the other dimer. The presence of these “rattlers” near $T^* = 0$ will depend on the geometrical parameters of the system, N , λ , and R . They are the result of a lack of bonds to maintain rigidity as required by the Maxwell criteria which is a global relation that stipulates that the number of zero modes, n_m , present in an arbitrary mechanical structure, is simply given by the difference between the number of degrees of freedom minus the number of independent constraints [46]. For a system with N particles in d dimensions subjected to N_c constraints the Maxwell criteria reads

$$n_m - n_{ss} = dN - N_c, \quad (2)$$

where n_{ss} is the number of redundant constraints or states of self-stress. For example, the structures with $E = 0, \epsilon, 2\epsilon, 3\epsilon$, and 6ϵ in Fig. 2 a) have $N_c = 5$ constraints and no redundant constraints, $n_{ss} = 0$. Four of the constraints originates from the direct interactions between the particles and one from the condition that the particles are confined touching the inner border of the common circular box. Accordingly, the Maxwell criterion gives $n_m = 3$ which corresponds to the three trivial modes: two independent translations and a global rotation, thus, all these structures are rigid. On the other hand, the structure with $E = 4\epsilon$ have $N_c = 4$ constraints, two of them arise from the internal bonds in the form of two identical dimers and two from the constraint that the centers of the dimers coincide as a result of being in a common box. Consequently, $n_m = 4$, from which three correspond to the trivial modes and one to a non-trivial mode corresponding to the relative rotation of one dimer with respect to the other as indicated by the green arrows. Although the configurations shown in Fig. 2 correspond to the more compact representatives for a given energy, other configuration with the same energy can not be excluded. Fig. 2 b) shows the free energy at zero temperature for different values of the box size. The free

energy curve shows steps that correspond to the number of corona overlaps for a given confining box size R . The most compact representative configurations for each energy are shown in the inserted drawings. The orange lines in the insets highlights the particles that overlap their coronas.

In Fig. 3 we show a phase diagram in the plane temperature vs box radius. This diagram shows that at high temperatures the particles move inside the box randomly without adopting a particular structure, except at small R . As T is lowered, the system abruptly adopts its final self-assembled structure for which the energy remains constant under further cooling. Notice that there exists small regions showing reentrant melting (around $k_B T/\epsilon \simeq 0.10$) for which an increase in R may lead from an ordered structure to a fluid like phase to another ordered structure. When the system is very small, which for the example shown, occurs at sizes $R \lesssim 2$, there is not enough room for the particles to move more or less freely since they are sterically constrained by the presence of the hard cores of the other particles, and the confining box. This is a reminiscence of the athermal behavior of hard discs since no change in the number of corona overlaps is possible at any temperature for these box sizes.

In Fig. 4, we identify the most compact representatives of the minimum energy configurations for systems with $\lambda = 2$ and $N \leq 6$. The energy of each configuration is indicated as well as the theoretical values of the box radius corresponding to each compact representative, as obtained by geometrical considerations. As expected, the structural complexity increases with N . Some of these configurations correspond to rigid structures, while others present rattlers, that is, particles that may change their relative positions to other particles in spite of being the more compact representative for its energy, while maintaining the energy of the configuration constant. To mention just a few of the non-rigid structures, for $N = 3$, the third configuration shows a rattler while for $N = 6$, the first, third, fourth, eighth, and ninth configurations show rattlers. Rattlers are highlighted by green dots (or a green line in the case of a dimer) and non-rigid structures are indicated by the blue panels. Notice that the configurations with $E = 0$ are analogous to those corresponding to confined hard disks with diameter $\lambda\sigma_0$. One may expect the same equivalence would be observed for the most compact cases as compared to hard disks with diameter σ_0 . This is true for the cases with $N = 1$ to 5 but for $N = 6$ the most compact configuration has no equivalent in the hard-disks case. This is due to the fact that the coronas of particles located on opposite sides of the confining box provide extra constraints that avoid the peripheral disks to rotate in contrast with the case with $N = 6$ and $E = 0$.

Low energy configurations for other values of N larger than 6 have also been considered, however, given the large variety and the complexity of the structures arising upon increasing N , we have not attempted to enumerate them. In fact, more sophisticated algorithms than the one used in this work would be necessary to thoroughly explore the energy landscape in search of a global minimum. In Fig. 5 we show interesting representatives for larger values of N , as indicated. For large number of particles we observe the formation of concentric shells of overlapping disks. This behavior is similar to the formation of concentric shells

obtained in the case of softly repulsive particles confined in a spherical box [47]. As the radius of the confining box decreases, these shells are intercalated with approximately uniformly distributed particles as seen in the last figure of the top panel. Residual defects are seen in this figure. It is possible to control to certain extent the resulting structure by an appropriate choice of the number of particles, the width of the corona, and the radius of the confining box as shown in the lower panel of Fig. 5. Here, the parameters were chosen specifically in order to obtain a sequence of configurations with different rotational symmetry or more precisely, with an increasing number of *compartments*, from one to six.

Figure 6 shows the free energy vs box size for large systems ($N = 100, 200$, and 400) in the normalized axis, $E/(N\epsilon)$ vs $R^2/(N\sigma_0^2)$. The symbols correspond to simulation results. Note that in these axes all the curves collapse in a single universal curve and this curve presents piecewise behavior with approximately linear sections. Different regions correspond to different arrangements of the particles. For example, for large R , the box is so large that no overlaps between coronas exist and the energy of the system is zero. Then, at $R^2/(N\sigma_0^2) \simeq 1.44$ the number of corona overlaps increase progressively as R decreases. The inset labeled (a) shows schematically a group of particles, some of them overlap with the nearest neighbors and some other do not overlap, forming lines similar to the ones shown for the case $N = 100$ and $E = 98\epsilon$ in Fig. 5 (a). A simple model can be proposed to describe the behavior in this regime. Let us imagine that the particles form a straight line of length $L = N_0\lambda\sigma_0 + N_1\sigma_0$ and width $W = \lambda\sigma_0$, where N_0 the number of particles that do not overlap and N_1 the number of particles that overlap with their neighbors, so that $N = N_0 + N_1$. The area fraction $\phi_1(N_1)$ of disks with diameter $\lambda\sigma_0$ in the rectangle of area WL is

$$\phi_1(N_1) = \frac{N \frac{\pi \lambda^2 \sigma_0^2}{4}}{\alpha W L} = \frac{N \pi \lambda}{4 \alpha [\lambda N + (1 - \lambda) N_1]}, \quad (3)$$

where α is a factor that takes into account the fact that the disks can not cover completely the rectangular stripe. This region starts at $\phi_1(N_1 = 0) \equiv \phi_0$, with ϕ_0 the maximum packing of disks without overlaps. This quantity is then

$$\phi_0 = \frac{N \frac{\pi \lambda^2 \sigma_0^2}{4}}{\pi R_0^2}, \quad (4)$$

where R_0 is the radius of the confining box when the overlaps start to appear. Using Eqs. (3) and (4) we get

$$\phi_1(N_1) = \frac{N^2 \lambda^3 \sigma_0^2}{4 R_0^2 [\lambda N + (1 - \lambda) N_1]}. \quad (5)$$

In general

$$\phi_1(N_1) = \frac{N \frac{\pi \lambda^2 \sigma_0^2}{4}}{\pi R^2}, \quad (6)$$

so that using Eqs. (5) and (6) and since $E = N_1 \epsilon$ then

$$\frac{E}{N\epsilon} = \frac{\lambda}{\lambda - 1} \left(1 - \frac{R^2}{R_0^2} \right), \quad (7)$$

where $\lambda \leq 2$ is being assumed. This regime ends at R_1 , when $N_1 = N$, so that all particles overlap and further shrinking of the box will produce more compact configuration like lines with kinks or branching points. From Eq. (7) we get $R_1 = R_0/\sqrt{2}$. From the simulation results, $R_0^2/(N\sigma_0^2) \simeq 1.44$, that once inserted in the model given by Eq. (7) and using $\lambda = 2$ gives the blue line in Fig. 6. Thus, the model reproduces correctly the simulation results.

The next regime consists of N_1 particles that overlap with their next neighbors in the line and N_2 kinks or branching points that has an extra overlap as shown in inset (b) of Fig. 6. The total number of particles is $N = N_1 + N_2$. Proceeding as before, let us assume that the particles are contained in a rectangular region of length $L = N_1\sigma_0 + \mu\sigma_0 N_2$ and width $W = \lambda\sigma_0$, with μ a fitting parameter that has to be introduced since kinks contribute less to the length of the rectangle such that $\mu < 1$. As before, the area fraction $\phi_2(N_2)$ of disks in the rectangle of area WL is

$$\phi_2(N_2) = \frac{N \frac{\pi \lambda^2 \sigma_0^2}{4}}{\alpha_2 WL} = \frac{N \pi \lambda}{4 \alpha_2 [N + (\mu - 1) N_2]}, \quad (8)$$

where again α_2 takes into account the fact that the rectangular stripe can not be completely covered by the disks. From the condition $\phi_2(N_2 = 0) = \phi_1(N)$ we get $\alpha_2 = \alpha$ and

$$\phi_2(N_2) = \frac{N^2 \lambda \sigma_0^2}{[N + (\mu - 1) N_2] R_0^2}. \quad (9)$$

Now, the free energy $E = (N_1 + 2N_2) \epsilon = (N + N_2) \epsilon$, and using Eq. (6), with $\phi_2(N_2)$ replacing $\phi_1(N_1)$ and Eq. (9) we get

$$\frac{E}{N\epsilon} = 1 + \frac{1}{1 - \mu} \left(1 - \frac{4R^2}{\lambda R_0^2} \right), \quad (10)$$

where again, $\lambda \leq 2$ is being assumed. In Fig. 6 we show with yellow line (b) the predictions of Eq. (10) with $R_0^2/(N\sigma_0^2) \simeq 1.44$, $\lambda = 2$, and the fitting parameter set to $\mu \simeq 0.76$. The rest of the curve grows more rapidly due to the increase in the number and the coordination number of the branching points as the box shrinks further.

4 Conclusions

In this paper we explored the phase behavior of model colloidal particles interacting via a core-corona potential confined inside a circular box. Specifically, we analyze how structural diversity depends on the size of the confining box

for a particular choice of the potential parameters. For small number of particles ($N \leq 6$), we identify the configurations establishing global energy minima and compare the results to the global minima corresponding to hard disks. We show that unlike the hard disks, for the same number of particles the system presents more than one global minimum depending on the radius of the confining cage and that in some cases the minimum-energy configurations contain rattlers, that is, particles that can move freely in a restricted region without changing the global minimum energy. Also, we have found that the presence of the coronas, confers stability to configurations that are not possible for hard disks. Interestingly, we obtain a large variety of open structures with diverse degree of anisotropy in spite of the isotropy of the interactions and of the confining box.

For large number of particles, the energy vs box radius curve shows the presence of well defined regimes characterized by the progressive appearing of branching points. Large confining boxes may allocate the particles without shoulder overlaps. As the size of the box decreases small strings start to appear up to the point of forming concentric rings without branches. At a certain point the box is so small that the particles can not be allocated unless branching points appear. The number of the branching points and the number of corona overlaps increase as the box size decreases finally reaching the most compact possible packing where all the particles form part of branching points.

The resulting assemblies can be considered as micro-structured particles with varying degree of complexity. Such particles suitably ordered on a surface can be used as a mask for patterning or directly as functional components for more complex structures.

Acknowledgements

We acknowledge partial financial support provided by DGAPA-UNAM through grant DGAPA IN-103419.

References

- [1] Rechtsman M., Stillinger F., and Torquato S., Designed interaction potentials via inverse methods for self-assembly, *Phys. Rev. E* **73**, 011406 (2006).
- [2] Rechtsman M., Stillinger F., and Torquato S., Synthetic diamond and wurtzite structures self-assemble with isotropic pair interactions, *Phys. Rev. E* **75**, 031403 (2007).
- [3] Min Y., Akbulut M., Kristiansen K., Golan Y., and Israelachvili J., The role of interparticle and external forces in nanoparticle assembly, *Nat. Mater.* **7**, 527 (2008).
- [4] Yethiraj A. and van Blaaderen A., A colloidal model system with an interaction tunable from hard sphere to soft and dipolar, *Nature* **421**, 513 (2003).

- [5] Tang C., Lennon E. M., Fredrickson G. H., Kramer E. J., Hawker C. J., Evolution of Block Copolymer Lithography to Highly Ordered Square Arrays, *Science* **322**, 429 (2008).
- [6] Wan D. and Glotzer S.C., Shapes within shapes: how particles arrange inside a cavity, *Soft Matter* **14**, 3012 (2018).
- [7] Marenduzzo D., Micheletti C., and Orlandini E., Biopolymer organization upon confinement, *J. Phys.: Condens. Matter* **22**, 283102 (2010).
- [8] Ellis R. J., Macromolecular crowding: obvious but underappreciated, *Trends Biochem. Sci.* **26**, 597 (2001).
- [9] Cines D. B., Lebedeva T., Nagaswami C., et. al., Clot contraction: compression of erythrocytes into tightly packed polyhedra and redistribution of platelets and fibrin, *Blood* **123**, 1596 (2014).
- [10] Hayashi T. and Carthew R. W., Surface mechanics mediate pattern formation in the developing retina, *Nature* **431**, 647 (2004).
- [11] Velev O. D., Lenho A. M., and Kaler E. W., A Class of Microstructured Particles Through Colloidal Crystallization, *Science* **287**, 2240 (2000).
- [12] Erin G. Teich, Greg van Anders, Daphne Klotsa, Julia Dshemuchadse, and Sharon C. Glotzer, Clusters of polyhedra in spherical confinement, *PNAS* **113**, E669 (2016).
- [13] Boles M. A., Engel M., and Talapin D. V., Self-Assembly of Colloidal Nanocrystals: From Intricate Structures to Functional Materials, *Chem. Rev.* **116**, 11220 (2016).
- [14] Manoharan V. N., Colloidal matter: Packing, geometry, and entropy, *Science* **349**, 1253751 (2015).
- [15] Burada P. S., Schmid G., Reguera D., Vainstein M. H., Rubi J. M., and Hanggi P., Entropic Stochastic Resonance, *Phys. Rev. Lett.* **101**, 130602 (2008).
- [16] Reguera D., Luque A., Burada P. S., Schmid G., Rubí J. M., and Hanggi P., Entropic Splitter for Particle Separation, *Phys. Rev. Lett.* **108**, 020604 (2012).
- [17] Sankaewtong K., Lei, Q., and Ni R., Self-assembled multi-layer simple cubic photonic crystals of oppositely charged colloids in confinement, *Soft Matter* **15**, 3104 (2019).
- [18] de Nijs B., et. al. Entropy-driven formation of large icosahedral colloidal clusters by spherical confinement, *Nature Materials* **14**, 56 (2014).

- [19] Wang D., et. al., Interplay between spherical confinement and particle shape on the self-assembly of rounded cubes, *Nature Communications* **9**, 2228 (2018).
- [20] Deißbeck F., Löwen H., and Oğuz E.C., Ground state of dipolar hard spheres confined in channels, *Physical Review E* **97**, 052608 (2018).
- [21] Löwen H., Twenty years of confined colloids: from confinement-induced freezing to giant breathing, *J. Phys.: Condens. Matter* **21**, 474203 (2009).
- [22] Schmidt M. and Löwen H., Phase diagram of hard spheres confined between two parallel plates, *Physical Review E* **55**, 7228 (1997).
- [23] Manoharan V. N. and Pine D. J., Building materials by packing spheres, *MRS Bulletin* **29**, 91 (2004).
- [24] Manoharan V. N., Colloidal spheres confined by liquid droplets: Geometry, physics, and physical chemistry, *Solid State Communications* **139**, 557 (2006).
- [25] Zhu X., Truskett T. M., and Bonnecaze R. T., Phase diagram for two-dimensional layer of soft particles, *Soft Matter* **15**, 4162 (2019).
- [26] Salgado-Blanco D. and Mendoza C. I., Non-additive simple potentials for pre-programmed self-assembly, *Soft Matter* **11**, 889 (2015).
- [27] Galisteo-López, J., Ibisate, M., Sapienza, R., FroufePerez, L., Blanco, A., and Lopez, C., Self-Assembled Photonic Structures, *Adv. Mater.* **23**, 30 (2011).
- [28] Stein A., Sphere templating methods for periodic porous solids, *Microporous Mesoporous Materials* **44**, 227 (2001).
- [29] Su, B.-L.; Sanchez, C.; Yang, X.-Y. *Hierarchically Structured Porous Materials: From Nanoscience to Catalysis, Separation, Optics, Energy, and Life Science*, 55129 (Wiley, 2012).
- [30] Souslov A., Liu A., and Lubensky T. C., Elasticity and Response in Nearly Isostatic Periodic Lattices, *Phys. Rev. Lett.* **103**, 205503 (2009).
- [31] Kapko V., Treacy M., Thorpe M., and Guest S., On the collapse of locally isostatic networks, *Proc. R. Soc. Lond. A* **465**, 3517 (2009).
- [32] Mao X., Souslov A., Mendoza C. I., and Lubensky T. C., Mechanical instability at finite temperature, *Nature Communications* **6**, 5968 (2015).
- [33] Madueno R., Räsänen M. T., Silien C., and Buck M., Functionalizing hydrogen-bonded surface networks with self-assembled monolayers, *Nature* **454**, 618 (2008).
- [34] Kravitz S., *Eng. Mater. Des.* **12**, 875 (1969).

- [35] Malescio G., Complex phase behaviour from simple potentials, *J. Phys.: Condens. Matter* **19**, 073101 (2007).
- [36] Denton A. in *Nanostructured Soft Matter*, A. V. Zvelindovsky, Ed. (Springer, Dordrecht, 2007), pp.395-436.
- [37] Norizoe Y. and Kawakatsu T., Monte Carlo simulation of string-like colloidal assembly, *Europhys. Lett.* **72**, 583 (2005).
- [38] Fomin T. D., Tsiok E. N., and Ryzhov V. N., The effect of confinement on the solid-liquid transition in a core-softened potential system, arXiv:1906.05780v1.
- [39] Malescio G. and Pellicane G., Stripe phases from isotropic repulsive interactions, *Nat. Mater.* **2**, 97 (2003).
- [40] Malescio G. and Pellicane G., Stripe patterns in two-dimensional systems with core-corona molecular architecture, *Phys. Rev. E* **70**, 021202 (2004).
- [41] Camp P. J., Structure and phase behavior of a two-dimensional system with core-softened and long-range repulsive interactions, *Phys. Rev. E* **68**, 061506 (2003).
- [42] Glaser M. A., Grason G. M., Kamien R. D., Kosmrlj A., Santangelo C. D. and Zihlerl P., Soft spheres make more mesophases, *Europhys. Lett.* **78**, 46004 (2007).
- [43] Fornleitner J. and Kahl G., Lane formation vs. cluster formation in two-dimensional square-shoulder systems —A genetic algorithm approach, *Europhys. Lett.* **82**, 18001 (2008).
- [44] Pauschenwein G. J. and Kahl G., Zero temperature phase diagram of the square-shoulder system, *J. Chem. Phys.* **129**, 174107 (2008).
- [45] Pauschenwein G. J. and Kahl G., Clusters, columns, and lamellae—minimum energy configurations in core softened potentials, *Soft Matter* **4**, 1396 (2008).
- [46] Maxwell, J. C., On the calculation of the equilibrium and stiffness of frames, *Phil. Mag.* **27**, 294 (1864).
- [47] Mughal A., Packing of Softly Repulsive Particles in a Spherical Box —A Generalised Thomson Problem, *Forma* **29**, 13 (2014).

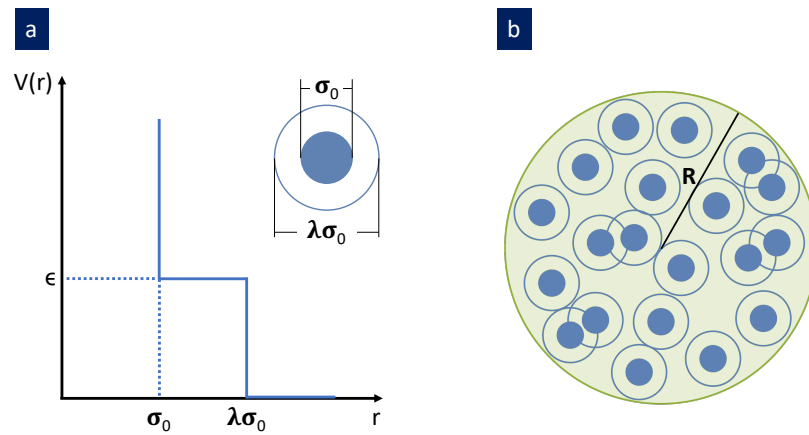


Figure 1: Description of the model. (a) The interaction between a pair of particles is modeled by a hard-core soft-corona potential. (b) A collection of particles confined in a circular box

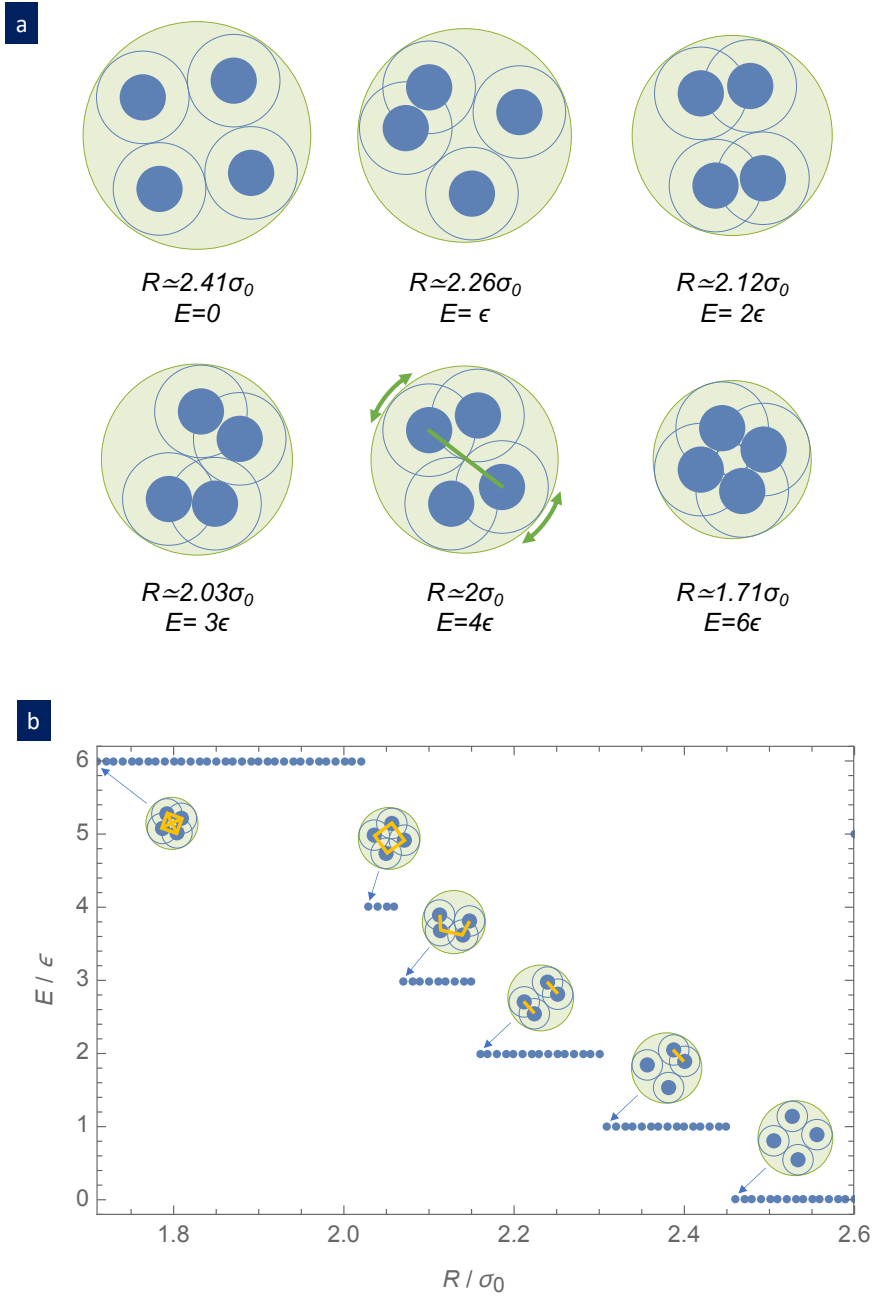


Figure 2: Representative minimum energy configurations for a system with four particles with $\lambda = 2$ and its energy diagram. (a) Most compact representative configurations for given values of the interaction energy. All the structures are rigid except for the case with $E = 4\epsilon$ which contain rigid dimers that move independently to each other in a certain region. One dimer is highlighted with a green line and the arrows indicate the movement of the dimer respect to the other. (b) As the size of the confining box is reduced, the number of corona overlaps increases and thus the energy increases in a stepwise fashion. The insets show the most compact representative for a given value of the energy. The yellow lines in the insets mark the pair of particles that participate in a given corona overlap. Therefore, the number of lines is the energy of the system. Notice that no configurations with five overlaps are allowed in this example.

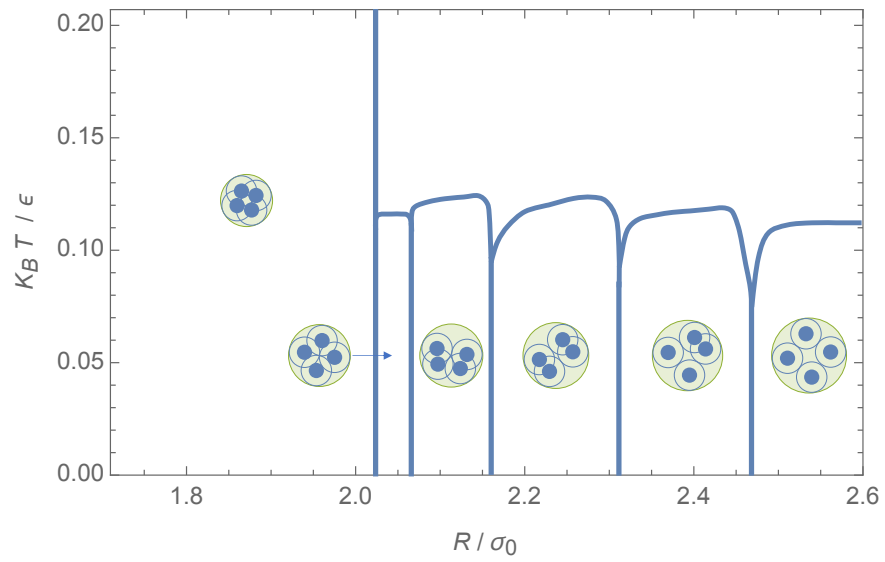


Figure 3: Temperature vs. box radius phase diagram for a system with four particles and $\lambda = 2$. The insets show the most compact representative for each minimum energy configuration.

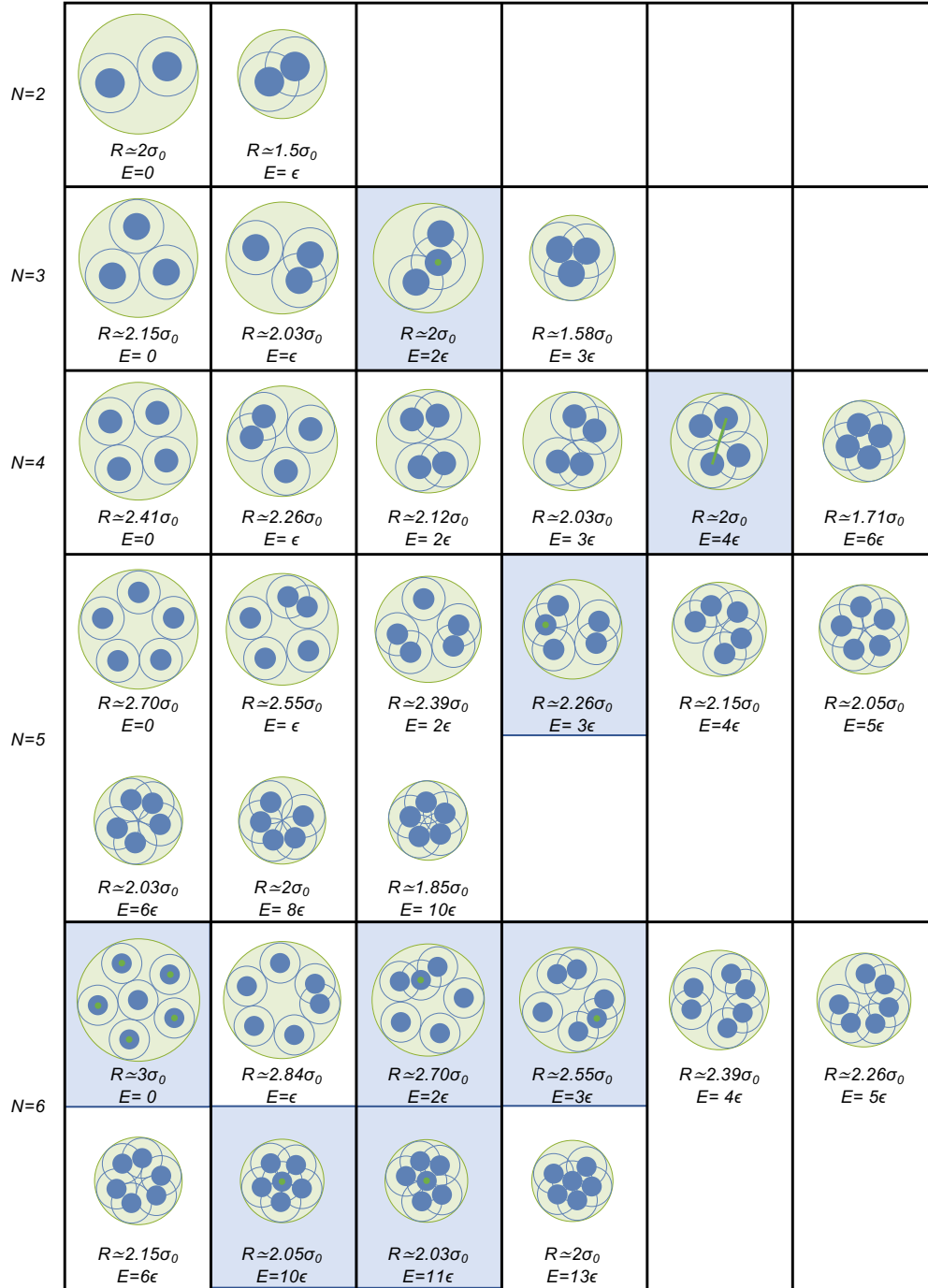


Figure 4: Representative minimum energy configurations for systems with a small number of particles and $\lambda = 2$. The number of configurations grows as the number of particle increases. Blue panels indicate non-rigid structures and the particles highlighted with a green dot are rattlers.

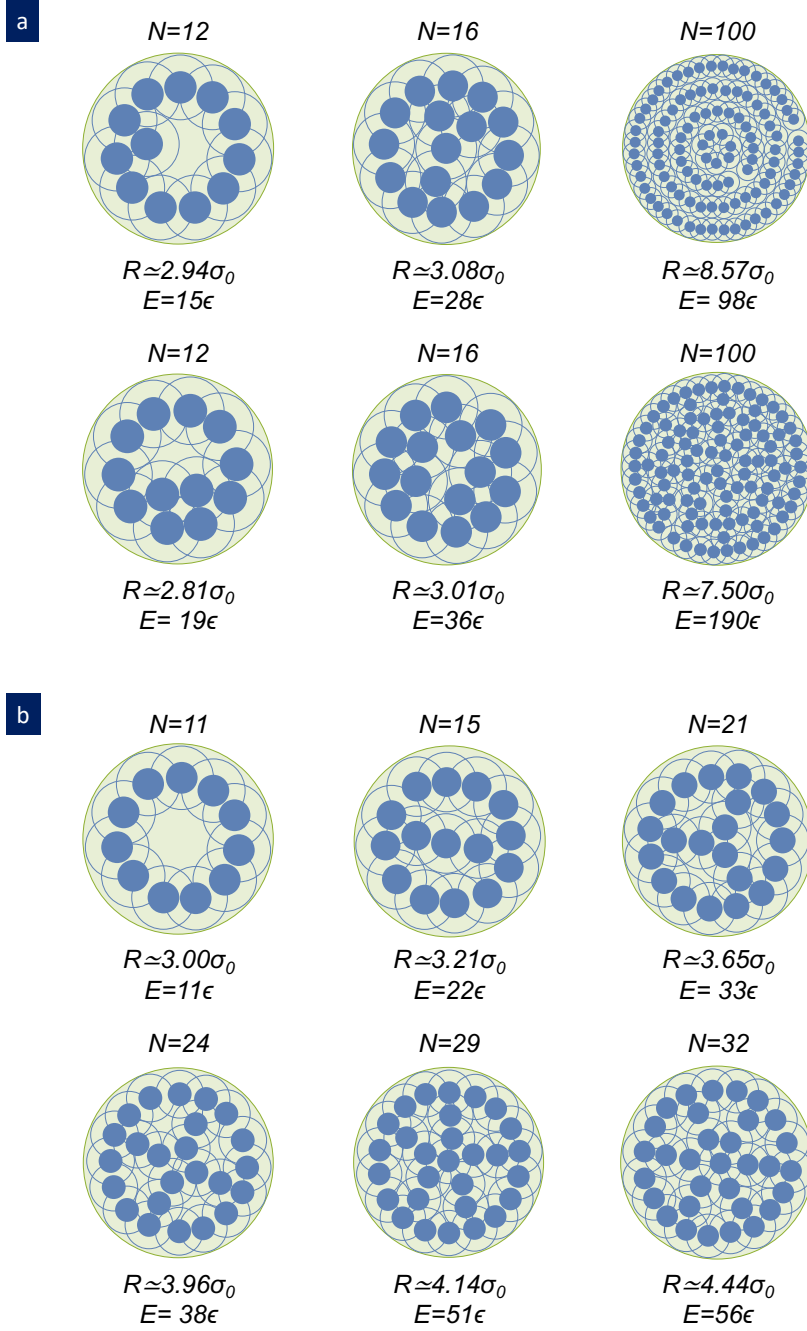


Figure 5: Other interesting configurations for systems with $\lambda = 2$. (a) Two representative configurations for each of $N = 12$, $N = 16$, and $N = 100$ particles. (b) Structured *microparticles* with a progressive number of *compartments*.

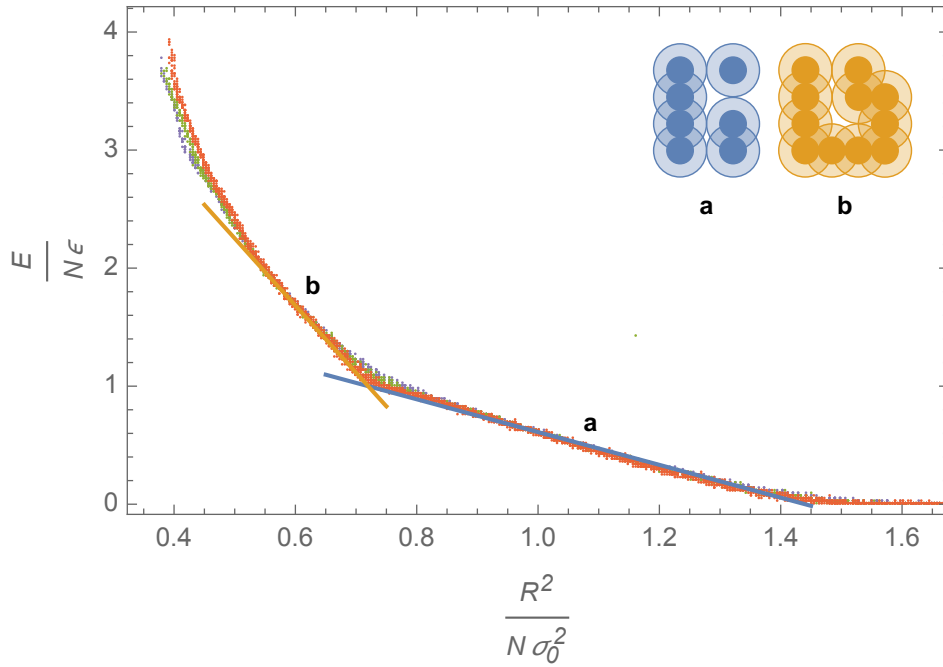


Figure 6: Pathway towards close packing. As the size of the confining box is reduced, the number of corona overlaps increases and thus the energy increases in a piecewise fashion as a consequence of the consecutive sequence of progressively denser and more branched configurations. An schematics of the first two sequential configurations present are shown in the inset. Symbols are simulation result with $N = 100$ (orange), $N = 200$ (green), and $N = 400$ (purple). The lines are the results of the models given by Eqs. (7) (blue) and (10) (yellow).